Automated IVS Reference Point Monitoring - First Experience from the Onsala Space Observatory

C. Eschelbach, R. Haas, M. Lösler

Abstract The realization of the International Terrestrial Reference Frame (ITRF) builds upon a combination of results derived from several geodetic space techniques, such as Very Long Baseline Interferometry (VLBI), Satellite and Lunar Laser Ranging (SLR and LLR) or Global Navigation Satellite Systems (GNSS). To combine the different techniques and their results in a meaningful way, co-location sites are important where equipment for several techniques is located reasonably close to each other. The relative geometries (local tie vectors) between the geometric reference points of the different techniques can be derived by terrestrial survey at these co-location sites. Within the Global Geodetic Observing System (GGOS) the requirements in terms of e.g. accuracy and frequency of local survey campaigns have been increased to guarantee that the local tie vectors reach an utmost level of global accuracy. In response to this request we developed a concept to achieve automated and continuous monitoring of radio telescope reference points. This concept was realized and tested in 2012 at the Onsala Space Observatory where an automated monitoring system was installed for a continual determination of the reference point of the 20 m radio telescope. The results confirm that uncertainties on the sub-mm level can be achieved with this approach. Furthermore, a recursive estimation method is suggested for continual determinations of the reference point position that form the basis of time series of local tie vectors.

Keywords VLBI, Radio Telescope, Reference Point Determination, Monitoring, Error Budget

Cornelia Eschelbach
cornelia.eschelbach@fb1.fh-frankfurt.de
University of Applied Sciences Frankfurt, Nibelungenplatz 1, DE-60318 Frankfurt am Main, Germany

Rüdiger Haas
rudiger.haas@chalmers.se
Chalmers University of Technology, Onsala Space Observatory SE-439 92 Onsala, Sweden

Michael Lösler
michael.loesler@bkg.bund.de
Bundesamt für Kartographie und Geodäsie Frankfurt, Richard-Strauss-Allee 11, DE-60598 Frankfurt am Main, Germany

1 Motivation

Frequent and accurate surveys of the reference points of space geodetic equipment at geodetic co-location stations is a challenging task for metrology-engineers. It is the basis for local tie vectors of an utmost level of accuracy that are necessary to guarantee meaningful multi-technique combinations within GGOS. Automated and continuous monitoring are desired to reduce time-consuming field work. The monitoring system HEIMDALL was developed and tested for an automated and continuous determination of the IVS reference point of the 20 m radio telescope at the Onsala Space Observatory in 2012.

2 Concept of Automated Reference Point Determination

In standard monitoring the motions or deformations of the observed object are directly related to the observed points that are fixed on the object. A radio telescope reference point that is located somewhere in the telescope structure cannot be observed directly but needs to be derived in an indirect way based on observations to points fixed on the moving parts of the telescope. In contrast to a standard monitoring, an automated reference point determination is an ambitious metrological challenge, because the observed points change their

positions as a function of the azimuth α and elevation angles ϵ of the radio telescope. Thus, a JAVA-based monitoring software was developed that considers the specific conditions of an automated reference point determination. Basically, the concept can be divided into four sub-tasks: the determination of a-priori positions, the network adjustment, the reference point determination, and the analysis of time series (cf. Lösler et al. (2013a)).

2.1 Determination of a-priori positions

From an operational point of view an automated monitoring should be carried out ideally during a regular VLBI session. The predicted positions of the mounted targets $\mathbf{P}^i_{\mathrm{Obs}}(\alpha,\epsilon)$ have to be derived from the VLBI schedule and from a-priori information concerning the local site network. Furthermore, a verification of the measurability of the predicted positions $\mathbf{P}^i_{\mathrm{Obs}}(\alpha,\epsilon)$ is necessary to reduce unneeded total station activities. The predicted position is expressed by

$$\mathbf{P}^i_{\mathrm{Obs}}(\alpha,\epsilon) = \mathbf{P}^0_{\mathrm{RP}} + \mathbf{R}_{\alpha,\epsilon}(\mathbf{P}^i_{\mathrm{Obs}} - \mathbf{P}^0_{\mathrm{RP}}) \tag{1}$$

where $\mathbf{R}$ denotes a rotation matrix, $\mathbf{P}^i_{\mathrm{Obs}}$ is the initial position of the mounted target observed at $\alpha = \epsilon = 0$, and $\mathbf{P}^0_{\mathrm{RP}}$ is an approximate position of the reference point. In addition to the initial position $\mathbf{P}^i_{\mathrm{Obs}}$, the normal direction vector $\mathbf{n}^i_{\mathrm{Obs}}$ of the prism has to observed to be able to determine the angle of incidence δ at the i^{th} target with respect to the survey point $\mathbf{P}_{\mathrm{TS}}$

$$\cos\tau^i = \frac{[\mathbf{P}_{\mathrm{TS}} - \mathbf{P}^i_{\mathrm{Obs}}(\alpha,\epsilon)]^T \mathbf{R}_{\alpha,\epsilon}\mathbf{n}^i_{\mathrm{Obs}}}{|\mathbf{P}_{\mathrm{TS}} - \mathbf{P}^i_{\mathrm{Obs}}(\alpha,\epsilon)||\mathbf{n}^i_{\mathrm{Obs}}|} \tag{2}$$

This angle of incidence has to be smaller than the specified opening angle of the used prism type to verify the accessibility.

2.2 Network Adjustment

The first analysis step is a common spatial network adjustment based on a Gauß-Markov model (e.g. Koch (2007)). For this purpose, the network adjustment combines the measured data and delivers the coordinates of the points at the telescope structure $\mathbf{P}^i_{\mathrm{Obs}}(\alpha,\epsilon)$ and their variance-covariance-matrix. If some of the $\mathbf{P}^i_{\mathrm{Obs}}(\alpha,\epsilon)$ are observed redundantly, outlier detection is possible within the network adjustment, and variance-component-estimation can be used to derive the uncertainties. In any other case, mismeasurements must be detected within the reference point determination in the next step. Furthermore, the estimated variance factor has only a limited validity and the derived variance-covariance-matrix is strongly depended on the a-priori stochastic model used in the network adjustment.

2.3 Reference Point Determination

We restrict the discussion on azimuth-elevation type radio telescopes, because most of the radio telescopes that are used for geodetic VLBI in the framework of the International VLBI Service for Geodesy and Astrometry (IVS) are of this type. The reference point of these radio telescopes is defined as the projection of the elevation axis on the fixed azimuth axis. Typically, the reference point is determined by indirect methods because it is not materialized. An often used method to estimate the reference point is based on circle fitting (Eschelbach and Haas (2003)) and was adopted by several groups (e.g. Dawson et al. (2007), Leinen et al. (2007)). Spatial circles result from a predefined observation configuration, fixing one axis while turning the other. Thus, the method is not suitable for a monitoring during normal operations of the radio telescope. For normal operations, Lösler's transformation model is an applicable alternative (Lösler (2009)):

$$\mathbf{P}_{\mathrm{Obs}} = \mathbf{P}_{\mathrm{RP}} + \mathbf{R}^{\mathbf{x}}_{\theta}\mathbf{R}^{\mathbf{y}}_{\phi}\mathbf{R}^{\mathbf{z}}_{\alpha-\mathbf{O}_\alpha}\mathbf{R}^{\mathbf{y}}_{\psi}(\mathbf{E_{cc}} + \mathbf{R}^{\mathbf{x}}_{\epsilon-\mathbf{O}_\epsilon}\mathbf{P}_{\mathrm{Tel}}) \tag{3}$$

where $\mathbf{P}_{\mathrm{Tel}} = [b\,a\,0]^T$ is a point in the telescope system, $\mathbf{E_{cc}}$ denotes the axis-offset, and the angle ψ describes the non-orthogonality between the azimuth- and elevation-axes. The vertical misalignment of the azimuth-axis is parameterized by θ and ϕ, and O_α and O_ϵ are additional orientation angles. This model has been adapted by Kallio and Poutanen (2012) by reformulating the rotation matrices in a commutative way (c.f. Nitschke and Knickmeyer (2000)). Nevertheless, both notations are equivalent and fulfill the requirements for an automated reference point monitoring. The positions $\mathbf{P}^i_{\mathrm{Obs}}(\alpha,\epsilon)$ and their related azimuth angles α and elevation angles ϵ are fitted to the described model that delivers the reference point and additional parameters like the axis-offset in an orthogonal distance fit (e.g. Eschelbach and Lösler (2012)). Outliers can be identified during the adjustment process of the reference point determination using multiple statistical tests (Lösler (2009)).

2.4 Time Series Analysis

In general, the results of a single survey epoch will be treated as invariant until a new measurement is carried out. In most cases the repeat-rate for a reference point determination is on the order of one or two years (cf. Klügel et al. (2011), Sarti et al. (2013)). Therefore, seasonal variations or abrupt changes can hardly be detected. More frequent reference point determinations result from an automated monitoring and advanced analyses are possible. The results of m reference point determinations $\mathbf{x_j}$ and their corresponding variance-covariance-matrices $\mathbf{Q_{x_j x_j}}$ can be combined by introducing recursive parameter estimation (cf. Koch (2007), Lösler et al. (2013a)).

$$\hat{\mathbf{x}}_j = \hat{\mathbf{x}}_{j-1} + \mathbf{K}_{j-1,j}(\mathbf{x}_j - \hat{\mathbf{x}}_{j-1}) \tag{4}$$

with the gain matrix

$$\mathbf{K}_{j-1,j} = \mathbf{Q}_{\hat{\mathbf{x}}_{j-1}\hat{\mathbf{x}}_{j-1}}(\mathbf{Q}_{\mathbf{x}_j\mathbf{x}_j} + \mathbf{Q}_{\hat{\mathbf{x}}_{j-1}\hat{\mathbf{x}}_{j-1}})^{-1} \tag{5}$$

The variance-covariance-matrix $\mathbf{Q}_{\hat{\mathbf{x}}_j\hat{\mathbf{x}}_j}$ follows with (e.g. Koch (2007))

$$\mathbf{Q}_{\hat{\mathbf{x}}_j\hat{\mathbf{x}}_j} = \mathbf{Q}_{\hat{\mathbf{x}}_{j-1}\hat{\mathbf{x}}_{j-1}} - \mathbf{K}_{j-1,j}\mathbf{Q}_{\hat{\mathbf{x}}_{j-1}\hat{\mathbf{x}}_{j-1}} \tag{6}$$

It is assumed, that a single determination is not invariant with time, thus an additional variance matrix of the process noise $\mathbf{C}_{\mathrm{nn}} = \mathrm{diag}(\dot{\sigma}^2_{x_{\mathbf{P}_{\mathrm{RP}}}} \dot{\sigma}^2_{y_{\mathbf{P}_{\mathrm{RP}}}} \dot{\sigma}^2_{z_{\mathbf{P}_{\mathrm{RP}}}})$ is introduced and delivers

$$\mathbf{Q}^{\Delta t}_{\mathbf{x}_j\mathbf{x}_j} = \mathbf{Q}_{\mathbf{x}_j\mathbf{x}_j} + \mathbf{B}\mathbf{C}_{\mathrm{nn}}\mathbf{B}^{\mathrm{T}} \tag{7}$$

The recursive parameter estimation enables the ongoing integration of the results of a current measurement epoch into a time series to achieve immediately reliable results.

2.5 Error Budget

Whereas random errors are handled by the stochastic model, systematic errors distort the results and have to be taken into account. In general, grouping the errors based on their sources is useful and can be depicted easily in an Ishikawa diagram (cf. Figure 1).

The telescope-dependent systematic errors are primarily the gravitational and thermal deformations. External sensors and specific observation strategies are needed to compensate for these deviations (e.g. Clark and Thomsen (1988), Haas et al. (1999), Sarti et al. (2011), Lösler et al. (2013b)). Systematic errors concerning the total station are mainly instrumental errors, e.g. encoder errors, trunnion axis error or horizontal collimation error (cf. Eschelbach and Lösler (2012)). Most of these errors are compensated by carrying out so-called two-face measurements as well as by applying reliable calibration values. In addition meteorology errors influence the scale parameter of the EDM-unit of the total station. Clock errors and time drifts have to be taken into account if time depending observations of different sensors are combined with each other. The stability and the configuration of the network affect the reliability of the measurement (cf. Abbondanza and Sarti (2012)).

Furthermore, the angle of incidence δ of a target beam from the total station's survey station point to the mounted glass-body prisms at the telescope varies as a function of α and ϵ. This causes a systematic displacement of the prism centre depending on the orientation of the prism relative to the total station. The radial derivation $\varepsilon_{\mathrm{radial}}$ and the lateral deviation $\varepsilon_{\mathrm{lateral}}$ are given by Pauli (1969)

$$\varepsilon_{\mathrm{radial}} = d\left(n - \sqrt{n^2 - \sin^2\delta}\right) - e(1 - \cos\delta) \tag{8}$$

and Rüeger (1990)

$$\varepsilon_{\mathrm{lateral}} = (d - e)\sin\delta - d\sec\delta_G \sin(\delta - \delta_G) \tag{9}$$

where $\delta_G = \arcsin\frac{\sin\delta}{n}$, e and d are the distance between the front surface of the prism and the apex and the corner point of the triple prism, respectively, and n denotes the refractive index ratio of glass and air.

Figure 2 depicts observed $\varepsilon_{\mathrm{radial}}$ and $\varepsilon_{\mathrm{lateral}}$ of a GPR121-type prism in a test setup (square and triangle markers), and for comparison the predicted values using Eq. (8) and Eq. (9), respectively. A misalignment of e.g. $\delta = 35°$ leads to deviations of $\varepsilon_{\mathrm{lateral}} = 1.2$ mm and $\varepsilon_{\mathrm{radial}} = 0.2$ mm. This means, if this is ignored it becomes a large contribution for the error budget of the point position. Unfortunately, this effect has never been taken into account in reference point determinations so far. The distance measurement can be corrected by

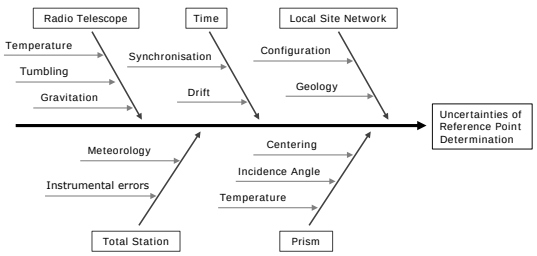

Fig. 1 Ishikawa-diagram for the error budget

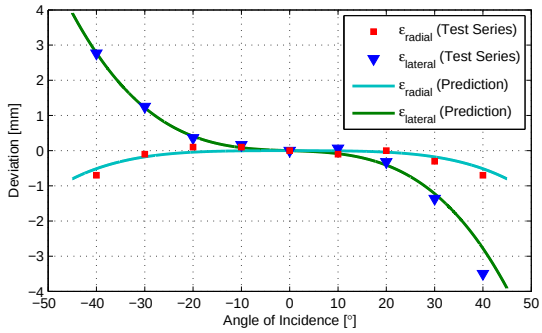

Fig. 2 Lateral and radial deviation for GPR121. The squares and triangles show measured radial and lateral deviations while the solid lines show the deviations according to equations 8 and 9.

adding $\varepsilon_{\text{radial}}$, but the lateral derivation $\varepsilon_{\text{lateral}}$ needs to be split-up into a horizontal and a vertical component. These components can be derived by a projection along the direction of the true position.

$$\mathbf{P}^{*}_{\text{Obs}} = \mathbf{P}^{i}_{\text{Obs}} - \frac{|\varepsilon_{\text{lateral}}|}{|\mathbf{q}^{i}_{\text{Obs}}|}\mathbf{q}^{i}_{\text{Obs}} \tag{10}$$

Here, the projection of the normal vector $\mathbf{n}_{\text{Obs}}$ into the observation plane is given by

$$\mathbf{q}^{i}_{\text{Obs}} = \mathbf{R}_{\alpha,\epsilon}\mathbf{n}^{i}_{\text{Obs}} - \left(\frac{[\mathbf{P}^{i}_{\text{Obs}} - \mathbf{P}_{\text{TS}}]^{T}\mathbf{R}_{\alpha,\epsilon}\mathbf{n}^{i}_{\text{Obs}}}{[\mathbf{P}^{i}_{\text{Obs}} - \mathbf{P}_{\text{TS}}]^{T}[\mathbf{P}^{i}_{\text{Obs}} - \mathbf{P}_{\text{TS}}]}\right)[\mathbf{P}^{i}_{\text{Obs}} - \mathbf{P}_{\text{TS}}] \tag{11}$$

If v and t are the estimated vertical and direction angles w.r.t. the observed point $\mathbf{P}_{\text{Obs}}$ and v^{*} and t^{*} are the estimated vertical and direction angles w.r.t. the projected position $\mathbf{P}^{*}_{\text{Obs}}$, respectively, the angle deviations are $\varepsilon_{\text{t}} = t^{*} - t$ and $\varepsilon_{\text{v}} = v^{*} - v$. This calculation can directly follow the measurements of the initial position and the normal direction vector of the prisms. The correction values are calculated in advance along with the observation plan so that the observations can be corrected already during the monitoring, just-in-time before being saved to the data base.

3 Monitoring Campaign at the Onsala Space Observatory

At the Onsala Space Observatory, four monitoring approaches (DMR, DMO, VMO and VSO) were carried out at the 20 m radio telescope using a high precision total station of type Leica TS30 and ten prisms of type GPR121 and GMP104.

The DMO-experiment was carried out twice, because it is assumed that a homogenous point cloud provides reliable results (cf. Table 1). Table 2 summarizes the smoothed results and their uncertainties derived from the analysis using eq. (4) – (7).

Table 1 Configurations of Survey Epochs.

Approaches/Experiment	**I**	**II**	**III**	**IV**	**V**
Dedicated survey/Real **V**LBI schedule	D	D	V	D	V
Single/**M**ultiple survey stand point(s)	M	M	M	M	S
Target was observed **O**nce/**R**edundantly	R	O	O	O	O

Table 2 'Smoothed' results from combining successive measurement campaigns.

Experiment	**I+II**	**I+II+III**	**I+...+IV**	**I+...+V**
$x_{\mathbf{P}_{\text{RP}}}$ [m]	90.1236	90.1236	90.1236	90.1236
	± 0.0002	± 0.0001	± 0.0001	± 0.0001
$y_{\mathbf{P}_{\text{RP}}}$ [m]	35.9493	35.9492	35.9492	35.9492
	± 0.0002	± 0.0002	± 0.0001	± 0.0001
$z_{\mathbf{P}_{\text{RP}}}$ [m]	22.7592	22.7592	22.7593	22.7592
	± 0.0002	± 0.0002	± 0.0002	± 0.0002
E_{cc} [mm]	−6.1	−6.1	−6.1	−6.0
	± 0.2	± 0.2	± 0.1	± 0.1

The smoothed results are presented in Figure 3 as green line with a 3σ error band, and the individual determinations based on the five experiments are shown as blue dots with 3σ error bars.

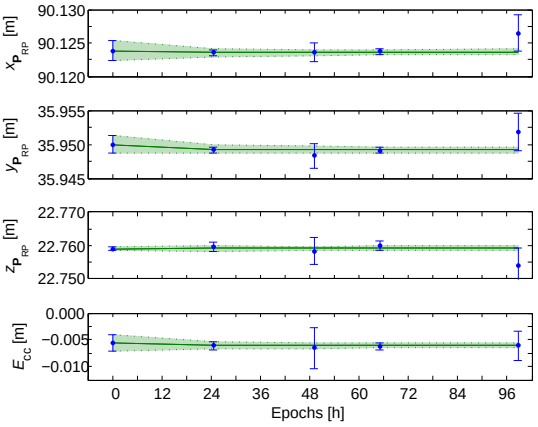

Fig. 3 Time series of the reference point coordinates and the telescope axis offset.

4 Conclusion

In 2012 the monitoring system HEIMDALL was installed for continuous observations of the IVS reference point of the 20 m radio telescope at the Onsala

Space Observatory. Five campaigns with different approaches were evaluated and combined by introducing a recursive parameter estimation. Furthermore, the use of glass-body prisms provides systematic errors up to the mm-level, which were for the first time considered by the authors for a reference point determination.

References

C. Abbondanza and P. Sarti. Impact of network geometry, observation schemes and telescope structure deformations on local ties: simulations applied to Sardinia Radio Telescope. *Journal of Geodesy*, **86**, 181–192, 2012.

T.A. Clark, P. Thomsen Deformations in VLBI antennas. Tech. rep., 100696, NASA, Greenbelt, MD, 1988.

J. Dawson, P. Sarti, G. Johnston, L. Vittuari. Indirect approach to invariant point determination for SLR and VLBI systems: an assessment. *Journal of Geodesy*, **81**, 433–441, 2007.

C. Eschelbach and R. Haas. The IVS-Reference Point at Onsala – High End Solution for a real 3D-Determination. In: *Proceedings of the 16th Meeting of the European VLBI Group for Geodesy and Astronomy*, 109–118, 2003.

C. Eschelbach and M. Lösler. Alternative ways for appropriate data analysis in industrial metrology. In: *Proceedings of the LowCost3D*, Deutsches Zentrum für Luft- und Raumfahrt, Berlin, 2012.

R. Haas, A. Nothnagel, H. Schuh, O. Titov. Explanatory supplement to the section 'Antenna Deformation' of the IERS Conventions (1996). In: *DGFI report nr. 71*, Deutsches Geodätisches Forschungsinstitut (DGFI), Munich (Germany), 26–29, 1999.

U. Kallio and M. Poutanen. Can We Really Promise a mm-Accuracy for the Local Ties on a Geo-VLBI Antenna. In: *Geodesy for Planet Earth*, International Association of Geodesy Symposia, 136, Springer-Verlag Berlin Heidelberg, 35–42, 2012.

K.R. Koch *Introduction to Bayesian Statistics*, Springer, Heidelberg/Berlin, 2nd edn., 2007.

T. Klügel, S. Mähler, C. Schade. Ground Survey and Local Ties at the Geodetic Observatory Wettzell. In: *17th Workshop on Laser Ranging*, Bad Kötzting, 2011.

S. Leinen, M. Becker, J. Dow, J. Feltens, K. Sauermann. Geodetic Determination of Radio Telescope Antenna Reference Point and Rotation Axis Parameters. *Journal of Surveying Engineering*, **133**, 41–51, 2007.

M. Lösler. New Mathematical Model for Reference Point Determination of an Azimuth-Elevation Type Radio Telescope. *Journal of Surveying Engineering*, **135**, 131–135, 2009.

M. Lösler, R. Haas, C. Eschelbach. Automated and Continual Determination of Radio Telescope Reference Points With Sub-mm Accuracy – Results from a campaign at the Onsala Space Observatory. *Journal of Geodesy* (Accepted for Publication), 2013a.

M. Lösler, A. Neidhardt, S. Mähler. Impact of Different Observation Strategies on Reference Point Determination – Evaluations from a Campaign at the Geodetic Observatory Wettzell. In: *Proceedings of the 21th Meeting of the European VLBI Group for Geodesy and Astronomy*, 2013b, this issue.

M. Nitschke, E.H. Knickmeyer. Rotation Parameters - A survey of Techniques. *Journal of Surveying Engineering*, **126**, 83–105, 2000.

W. Pauli. Vorteile eines kippbaren Reflektors bei der elektrooptischen Streckenmessung. *Vermessungstechnik*, 412–415, 1969.

J.M. Rüeger. *Electronic Distance Measurement - An Introduction*, Springer, Heidelberg/Berlin, 3rd edn., 1990.

S. Sarti, C. Abbondanza, L. Petrov, M. Negusini. Height bias and scale effect induced by antenna gravitational deformations in geodetic VLBI data analysis. *Journal of Geodesy*, **85**, 1–8, 2011.

S. Sarti, C. Abbondanza, J. Legrand, C. Bruyninx, L. Vittuari, J. Ray. Intrasite motions and monument instabilities at Medicina ITRF co-location site. *Geophys. J. Int.*, **192**, 1–10, 2013.